Article

Cell Metabolism

Long-Term Administration of Nicotinamide Mononucleotide Mitigates Age-Associated Physiological Decline in Mice

Graphical Abstract

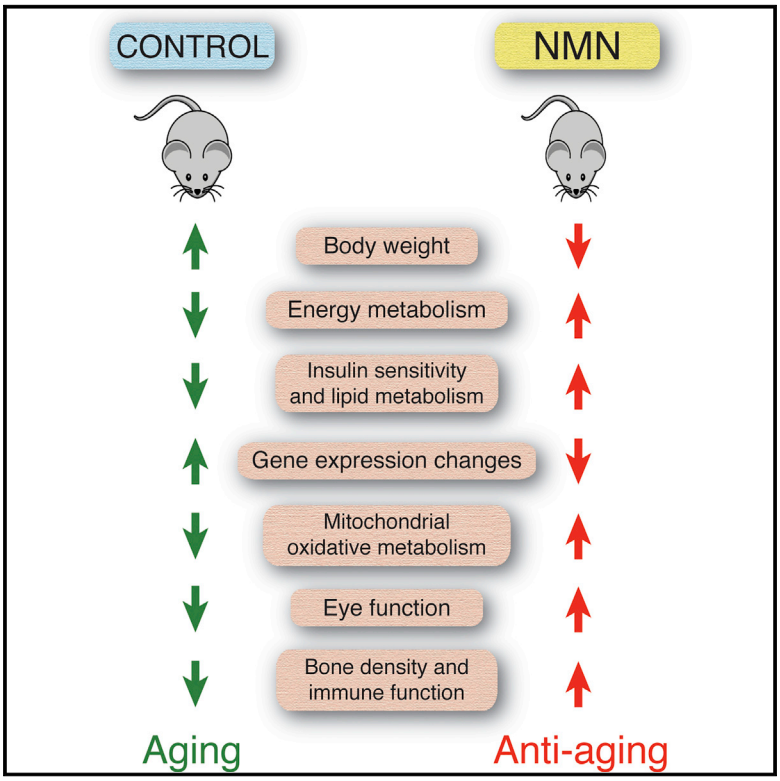

Highlights

- NMN suppresses age-associated body weight gain and enhances energy metabolism
- NMN improves insulin sensitivity, eye function, and other features with no toxicity
- NMN prevents age-associated gene expression changes in a tissue-specific manner
- NMN is an effective anti-aging intervention that could be translated to humans

Authors

Kathryn F. Mills, Shohei Yoshida, Liana R. Stein, ..., Koji Uchida, Jun Yoshino, Shin-ichiro Imai

Correspondence

jyoshino@wustl.edu (J.Y.), imaishin@wustl.edu (S.I.)

In Brief

Mills et al. conducted a 12-month-long administration of nicotinamide mononucleotide (NMN), a key natural NAD^+ intermediate, to normal wild-type mice, demonstrating that NMN effectively mitigates age-associated physiological decline in mice without any obvious toxicity. These results highlight the significant potential of NMN as an effective anti-aging intervention in humans.

Accession Numbers

GSE85718

Mills et al., 2016, Cell Metabolism *24*, 795–806
December 13, 2016
http://dx.doi.org/10.1016/j.cmet.2016.09.013

CellPress

Cell Metabolism
Article

Long-Term Administration of Nicotinamide Mononucleotide Mitigates Age-Associated Physiological Decline in Mice

Kathryn F. Mills,[1] Shohei Yoshida,[2] Liana R. Stein,[1,7] Alessia Grozio,[1] Shunsuke Kubota,[3] Yo Sasaki,[4] Philip Redpath,[5] Marie E. Migaud,[5] Rajendra S. Apte,[1,3] Koji Uchida,[2] Jun Yoshino,[6,*] and Shin-ichiro Imai[1,8,*]
[1]Department of Developmental Biology, Washington University School of Medicine, St. Louis, MO 63110, USA
[2]Oriental Yeast Company, Tokyo 174-0051, Japan
[3]Department of Ophthalmology
[4]Department of Genetics
Washington University School of Medicine, St. Louis, MO 63110, USA
[5]School of Pharmacy, Queen's University Belfast, Belfast, Northern Ireland BT7 1NN, UK
[6]Division of Geriatrics and Nutritional Science, Department of Medicine, Center for Human Nutrition, Washington University School of Medicine, St. Louis, MO 63110, USA
[7]Present address: Gladstone Institute of Neurological Disease and Department of Neurology, University of California, San Francisco, San Francisco, CA 94158, USA
[8]Lead Contact
*Correspondence: jyoshino@wustl.edu (J.Y.), imaishin@wustl.edu (S.I.)
http://dx.doi.org/10.1016/j.cmet.2016.09.013

SUMMARY

NAD^+ availability decreases with age and in certain disease conditions. Nicotinamide mononucleotide (NMN), a key NAD^+ intermediate, has been shown to enhance NAD^+ biosynthesis and ameliorate various pathologies in mouse disease models. In this study, we conducted a 12-month-long NMN administration to regular chow-fed wild-type C57BL/6N mice during their normal aging. Orally administered NMN was quickly utilized to synthesize NAD^+ in tissues. Remarkably, NMN effectively mitigates age-associated physiological decline in mice. Without any obvious toxicity or deleterious effects, NMN suppressed age-associated body weight gain, enhanced energy metabolism, promoted physical activity, improved insulin sensitivity and plasma lipid profile, and ameliorated eye function and other pathophysiologies. Consistent with these phenotypes, NMN prevented age-associated gene expression changes in key metabolic organs and enhanced mitochondrial oxidative metabolism and mitonuclear protein imbalance in skeletal muscle. These effects of NMN highlight the preventive and therapeutic potential of NAD^+ intermediates as effective anti-aging interventions in humans.

INTRODUCTION

Historically unprecedented worldwide trends in population aging are predicted to become an incessant burden on governmental healthcare finances (OECD, 2013). To make the process of aging healthy and prevent expensive age-associated health problems, efforts to develop effective, affordable, anti-aging interventions have recently been intensified, leading to some promising compounds, such as metformin, rapamycin, and SIRT1 activators (Barzilai et al., 2016; Hubbard and Sinclair, 2014; Lamming et al., 2013). Whereas these compounds were originally developed as pharmaceutical drugs, some endogenous compounds might also have the potential to achieve healthy and productive lives even at a very old age (Imai, 2010; Imai and Guarente, 2014).

Nicotinamide mononucleotide (NMN) and nicotinamide riboside (NR), key NAD^+ intermediates in mammals, could be such candidates (Imai, 2010). NMN is synthesized from nicotinamide (Nic), an amide form of vitamin B_3, and 5′-phosphoribosyl-pyrophosphate (PRPP) by nicotinamide phosphoribosyltransferase (NAMPT), the rate-limiting enzyme in this particular NAD^+ biosynthetic pathway (Cantó et al., 2015; Imai and Guarente, 2014). NR is phosphorylated to NMN by nicotinamide riboside kinases (NRKs) (Belenky et al., 2007). Once NMN is synthesized, it is converted to NAD^+ by three NMN adenylyltransferases, NMNAT1-3. The short-term administration of either NMN or NR has been reported to have remarkable therapeutic effects on metabolic complications and other disease conditions. For example, we have shown that NMN ameliorates impairments in glucose-stimulated insulin secretion in aged wild-type mice and some genetic mouse models (Ramsey et al., 2008; Revollo et al., 2007). NMN treatment also significantly improves both insulin action and secretion in diet- and age-induced type 2 diabetic or obese mouse models (Caton et al., 2011; Yoshino et al., 2011). Furthermore, NMN protects the heart from ischemia/reperfusion injury by preventing NAD^+ decrease induced by ischemia (Yamamoto et al., 2014), maintains the neural stem/progenitor cell population, and restores skeletal muscle mitochondrial function and arterial function in aged mice (de Picciotto et al., 2016; Gomes et al., 2013; Stein and Imai, 2014), ameliorates mitochondrial function, neural death, and cognitive

function in Alzheimer's disease rodent models (Long et al., 2015; Wang et al., 2016). NR is also able to ameliorate mitochondrial dysfunction in obese mouse models (Cantó et al., 2012; Gariani et al., 2015; Lee et al., 2015) and various mitochondrial disease models (Cerutti et al., 2014; Khan et al., 2014), attenuate cognitive deterioration in Alzheimer's disease model mice (Gong et al., 2013), prevent DNA damage and hepatocellular carcinoma formation (Tummala et al., 2014), improve noise-induced hearing loss (Brown et al., 2014), and maintain muscle stem cell function (Zhang et al., 2016). Collectively, these findings strongly suggest that enhancing NAD^+ biosynthesis by administering NMN or NR is an efficient therapeutic intervention against many disease conditions (Imai and Guarente, 2014).

Interestingly, it has been demonstrated that enhancing NAD^+ biosynthesis extends lifespan in yeast, worms, and flies (Anderson et al., 2002; Balan et al., 2008; Mouchiroud et al., 2013). In rodents and humans, a number of studies have reported that NAD^+ content declines with age in multiple organs, such as pancreas, adipose tissue, skeletal muscle, liver, skin, and brain (Gomes et al., 2013; Massudi et al., 2012; Mouchiroud et al., 2013; Stein and Imai, 2014; Yoshino et al., 2011; Zhu et al., 2015). Thus, enhancing NAD^+ biosynthesis with NMN or NR is expected to provide significant preventive effects on various pathophysiological changes in the natural process of aging. To address this critical question, long-term administration studies need to be performed under normal conditions in wild-type mice.

To examine whether long-term administration of NMN shows preventive effects on age-associated pathophysiological changes, we treated regular chow-fed wild-type mice for 12 months with two different doses of NMN in their drinking water. We assessed a variety of functional traits, as well as long-term safety and toxicity, and found that NMN is remarkably capable of ameliorating age-associated physiological decline in mice. Our findings from this long-term administration study provide a proof of concept to develop NMN as an effective anti-aging compound that prevents age-associated physiological decline, hoping to translate the results to humans.

RESULTS

Orally Administered NMN Increases Plasma NMN and Tissue NAD^+ Levels

In our previous study, we showed that a bolus intraperitoneal administration of NMN (500 mg/kg body weight) increased tissue NMN and NAD^+ levels within 15 min in the liver, pancreas, and white adipose tissue (WAT) in regular chow-fed wild-type mice (Yoshino et al., 2011). To make long-term NMN administration possible, we decided to test lower doses, which could potentially be translatable to humans, and add it to drinking water. We confirmed that 93%–99% of NMN was maintained intact in drinking water at room temperature for 7–10 days (Figure S1A). We next administered NMN at a dose of 300 mg/kg body weight to mice by oral gavage and measured plasma NMN and hepatic NAD^+ levels over 30 min. Plasma NMN levels exhibited a steep increase at 2.5 min, further increases from 5 to 10 min, and then went back to original levels at 15 min (Figure 1A), implicating very fast absorption in the gut. Consistent with this notion, hepatic NAD^+ levels showed a steady increase from 15 to 30 min (Figure 1A). We also measured tissue NAD^+ levels 60 min after oral gavage of NMN. Although differences did not reach statistical significance at this particular dose, relatively small increases in NAD^+ levels were observed in the liver, skeletal muscle, and cortex of the brain, but not in WAT or brown adipose tissue (BAT) (Figures 1B and S1B). To further confirm whether orally administered NMN is utilized to synthesize NAD^+ in tissues, we used doubly-labeled isotopic NMN (C13-D-NMN; Figure S1C) and traced these labels in NAD^+ in the liver and soleus muscle by mass spectrometry. Interestingly, in the liver, after administering C13-D-NMN by oral gavage, we clearly detected doubly labeled NAD^+ (C13-D-NAD^+) at 10 min, and the level of C13-D-NAD^+ further increased at 30 min (Figures 1C and S1D). In the soleus muscle, we detected C13-D-NAD^+ at 30 min, but not at 10 min (Figures 1C and S1D). These results suggest that orally administered NMN is quickly absorbed, efficiently transported into blood circulation, and immediately converted to NAD^+ in major metabolic tissues.

To determine the effects of long-term NMN administration on age-associated pathophysiologies, we performed a 12-month-long NMN administration study using regular chow-fed wild-type C57BL/6N mice (Figures 1D and S1E). We tested two doses of NMN, 100 and 300 mg/kg/day, from 5 months to 17 months of age. During this period, we carefully monitored the tolerance of mice to NMN by measuring water intake in control and NMN-administered mice and found that NMN administration was well tolerated over 12 months (see below). This long-term oral administration regimen could cause very small increases in the steady-state levels of plasma or tissue NMN and NAD^+ when mice take a sip of NMN-containing water. However, it is technically very difficult to detect such small fluctuations of plasma or tissue NMN and NAD^+ levels. Nonetheless, we observed a tendency of dose-dependent NAD^+ increase over time in the liver and BAT, but not in other tissues including skeletal muscle and WAT (Figure 1E).

NMN-Administered Mice Exhibit Suppression of Age-Associated Body Weight Gain

We next assessed a variety of physiological, biochemical, and molecular parameters in control and NMN-administered mice. We found that NMN administration significantly and dose-dependently suppressed age-associated body weight gain (Figures 2A and 2B). There was a statistically highly significant interaction between time and group ($p < 0.001$ from the two-way repeated-measures ANOVA). Additionally, the linear dose-dependent effects were statistically significant at all time points through 4–12 months ($p < 0.05$ from the one-way repeated-measures ANOVA with the unweighted linear term) (Figure 2A). The average numbers of percent body weight reduction normalized to control mice were 4% and 9% in 100 and 300 mg/kg/day groups, respectively. This suppressive effect of NMN on age-associated body weight gain became more evident by plotting body weight gain in each group (Figure 2B). Again, the interaction between time and group was statistically highly significant ($p < 0.001$ from the two-way repeated-measures ANOVA), and the linear dose-dependent effects were significant at all points through 2–12 months ($p < 0.01$ from the one-way repeated-measures ANOVA with

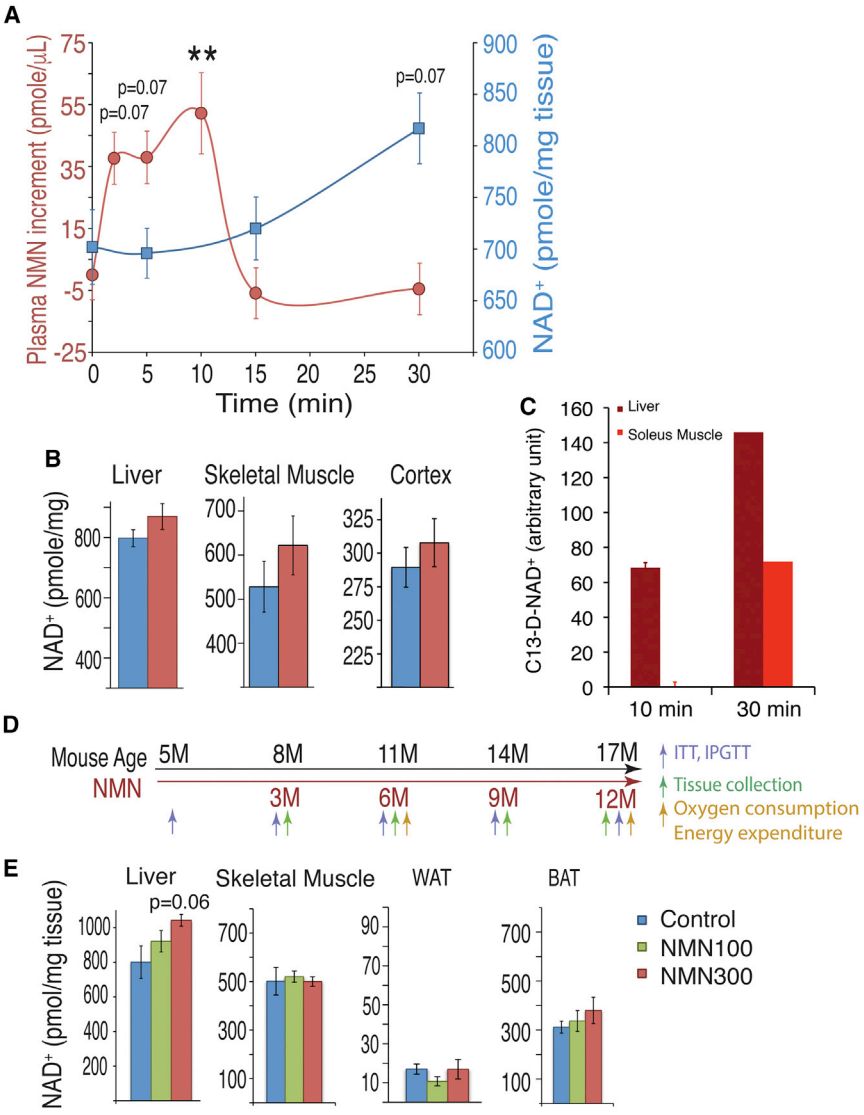

Figure 1. Oral Administration of Nicotinamide Mononucleotide Increases Plasma NMN and Tissue NAD+ Levels in Mice

Three- to four-month-old C57BL/6N mice were given nicotinamide mononucleotide (NMN) either by oral gavage (300 mg/kg) or ad libitum in the drinking water (100 or 300 mg/kg/day).

(A) Plasma NMN (red circles) and liver NAD^+ (blue squares) levels were measured by HPLC after oral gavage (300 mg/kg) (n = 5–13 per time point). **p < 0.01 compared to 0 min.

(B) NAD^+ levels 1 hr after oral gavage (300 mg/kg) in the liver, skeletal muscle, and cortex of control (blue) and NMN-administered (red) mice (n = 10 mice per group).

(C) Doubly-labeled isotopic NAD^+ (C13-D-NAD^+) were measured in the liver and soleus muscle by mass spectrometry at 10 and 30 min time points after orally administering doubly-labeled isotopic NMN (C13-D-NMN) (n = 3 at 10 min and n = 1 at 30 min). The areas under the curves of C13-D-NAD^+ were calculated by subtracting the background values of PBS controls.

(D) A scheme showing the long-term NMN administration and various analyses. NMN (100 or 300 mg/kg/day) was dissolved into the drinking water and administered ad libitum to C57BL/6N male mice for 12 months, starting at 5 months of age. Experiments were performed at intervals to document the changes over time, as indicated.

(E) NAD^+ was measured in the liver, skeletal muscle, white adipose tissue (WAT), and brown adipose tissue (BAT) of control (blue) and 100 (green) and 300 (red) mg/kg/day NMN-administered mice 6 months after NMN administration (at 11 months of age) (n = 4–5 per group). All values are presented as mean ± SEM.

the unweighted linear term). At 12 months, the 300 mg/kg/day group tended to have a decreased fat mass and an increased lean mass compared to controls (Figure S1F). NMN-administered and control mice did not show any recognizable difference in body length (Figure S2A). Interestingly, when mice became older, NMN-administered mice were able to maintain higher levels of food and water consumption in a dose-dependent manner compared to control mice (Figures 2C and 2D). These results confirm that the effect of NMN on body weight was not due to a growth defect or loss of appetite. Furthermore, analyses of blood cell counts (Figures S2B–S2E), blood chemistry panels (Figures S2F–S2W), and urine (Figure S2X) did not detect any sign of obvious toxicity from NMN at either dose. No statistical difference was detected by the log-rank test in survival of mice over the entire intervention period between control, 100 and 300 mg/kg/day NMN-administered mouse cohorts. No obvious differences were observed for the causes of death, which included urinary tract obstruction, thrombosis, and myocardial infarction, between control and NMN-administered mice (Figure S3A). These results suggest that NMN administration can significantly suppress age-associated body weight gain in a dose-dependent manner in regular chow-fed mice, without showing any serious side effects during the entire 12-month intervention period.

NMN-Administered Mice Show Enhancement of Energy Metabolism and Higher Physical Activity during the Dark Time

Because NMN-administered mice showed higher food intake but lower body weight compared to control mice during the process of aging, we measured oxygen consumption, energy expenditure, and respiratory quotient at the 6- and 12-month time points for control, 100, and 300 mg/kg/day NMN-administered mice (Figures 3A–3E). Oxygen consumption significantly increased in both 100 and 300 mg/kg/day groups during both light and dark periods (Figure 3A). Energy expenditure also showed significant increases through 24 hr in the 100 mg/kg/day group and during the light period in the 300 mg/kg/day group (Figure 3B). Respiratory quotient significantly decreased in both groups during both light and dark periods (Figure 3C), suggesting that NMN-administered mice switched their main energy

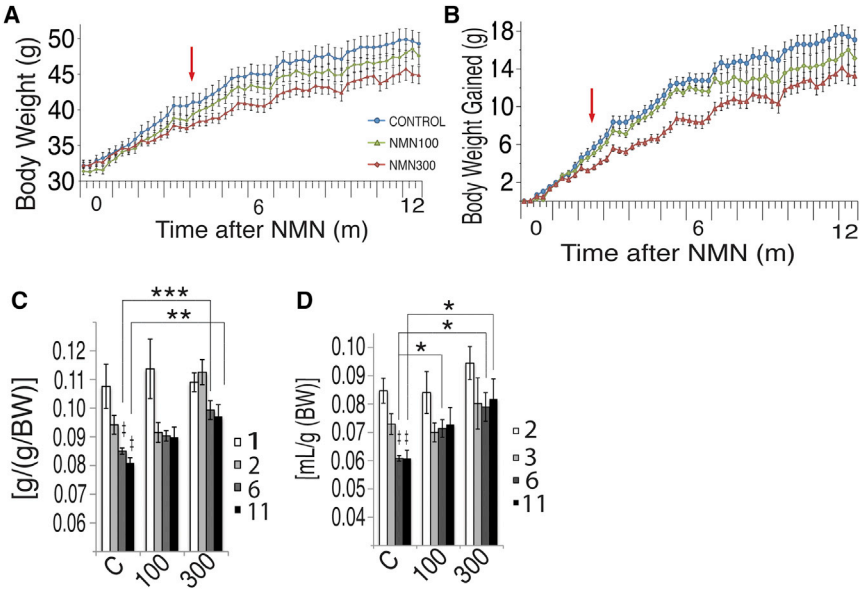

Figure 2. NMN-Administered Mice Exhibit Suppression of Age-Associated Weight Gain while Maintaining Food and Water Intake during the Process of Aging

Body weight and food and water intake were monitored throughout the 12-month intervention period in control (blue) and 100 (green) and 300 (red) mg/kg/day NMN-administered mice.

(A and B) Body weight (A) and body weight gain (B) were plotted for each group (n = 9–15 per group). Red arrows indicate the starting point for both the statistically significant differences between control and 300 mg/kg/day NMN groups ($p < 0.001$ from two-way repeated-measures ANOVA), and statistically significant dose-dependent effects ($p < 0.05$ [A] or $p < 0.01$ [B] from one-way repeated-measures ANOVA with the unweighted linear term).

(C and D) Food (C) and water intake (D) were measured throughout the 12-month intervention period. Symbol (‡) indicates statistically significant differences within control groups ($p < 0.05$); 6- and 11-month (dark gray and black bars, respectively) versus 1-month (white bar) in food intake, and 6- and 11-month (dark gray and black bars, respectively) versus 2-month (white bar) in water intake. Asterisks indicate statistically significant differences compared to controls at indicated time points (*$p < 0.05$, **$p < 0.01$, ***$p < 0.001$ by ANOVA with Tukey post hoc test; n = 9–15 per group). All values are presented as mean ± SEM.

source from glucose to fatty acids. Body temperature did not significantly change, although NMN-administered mice occasionally showed a tendency of higher body temperatures (Figure S3B). Interestingly, whereas oxygen consumption and energy expenditure significantly decreased, particularly during the dark period, from 6 months to 12 months in control mice, mice treated with NMN for 12 months were able to maintain both oxygen consumption and energy expenditure close to those of control mice at 6 months after NMN administration (Figures 3D and 3E). Taken together, these results strongly suggest that NMN has significant preventive effects against age-associated impairment in energy metabolism in regular chow-fed wild-type mice.

We also evaluated the general locomotor activity in control and NMN-administered mice at 12–15 months of age. Ambulations (whole-body movements) and rearing (vertical activity) were measured (Figures 3F and 3G). Compared to control mice, mice administered with 100 mg/kg/day NMN showed significantly higher hourly ambulations during the dark period, whereas mice administered with 300 mg/kg/day NMN showed slightly lower ambulations (Figure 3F). In rearing activity, there was no significant difference between control and 100 mg/kg/day groups (Figure 3G). However, the 300 mg/kg/day group exhibited decreases in rearing activity throughout the dark period (Figure 3G). Thus, whereas NMN administration can stimulate energy metabolism and general locomotor activity in aged mice, a lower dose appears to be optimal for these particular parameters.

NMN-Administered Mice Show Improved Insulin Sensitivity and Plasma Lipid Profile

We assessed the effect of NMN on glucose and lipid metabolism by conducting intraperitoneal glucose and insulin tolerance tests (IPGTTs and ITTs, respectively) and measuring plasma lipid panels at 3, 6, 9, and 12 months of treatment. To eliminate the possible confounding effects induced by body weight differences between control and NMN-administered mice (Figure 2A), we evaluated these metabolic parameters in body weight-matched groups of control and NMN-administered mice. We did not observe any significant differences in glucose tolerance among the control and the 100 and 300 mg/kg/day NMN-administered groups through all time points (Figure S4A). No difference was observed in plasma insulin levels during IPGTTs among three groups (Figure S4B). Fasted insulin levels increased over time in all three groups. However, the 300 mg/kg/day NMN-administered group tended to show lower fasted insulin levels after 3–9 months of treatment (Figure S4C). Interestingly, fed insulin levels showed a clearer tendency of lower insulin levels in NMN-administered groups compared to control groups (Figure S4D), whereas fed blood glucose levels were not different among three groups (Figure S4E). Consistent with these insulin results, after 12 months of NMN administration (mice were 17 months old), NMN-administered mice showed significantly improved insulin sensitivity compared to the body weight-matched control group (Figure 4A). There was a statistically significant interaction between time and group ($p = 0.023$ from the Greenhouse-Geisser test in two-way repeated-measures ANOVA), and the linear dose-dependent effects were statistically significant or close to significance at the 30 min and 45 min time points, respectively ($p = 0.026$ and $p = 0.061$ in the one-way repeated-measures ANOVA with unweighted linear term). This improved insulin sensitivity in the 100 and 300 mg/kg groups became more evident when plotting percent glucose changes relative to the glucose levels at 0 min time point (Figure 4B), although the interaction between time and group did not reach statistical significance in this assessment ($p = 0.091$ from the Greenhouse-Geisser test in two-way repeated-measures ANOVA). Similar improvement of insulin sensitivity was still

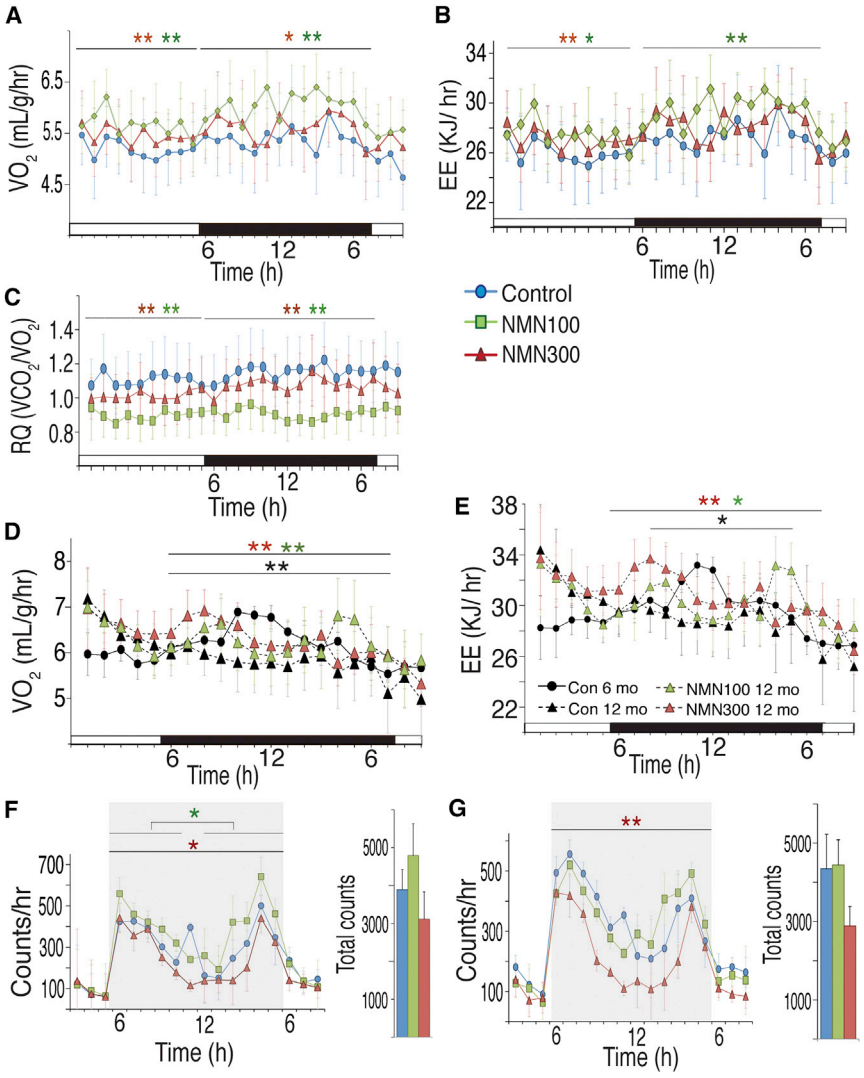

Figure 3. NMN-Administered Mice Show Enhancement of Energy Metabolism and Higher Physical Activity during the Dark Time

(A–C) Oxygen consumption (VO_2) (A), energy expenditure (EE) (B), and respiratory quotient (RQ) (C) were measured after 12 months of NMN administration using indirect calorimetry (n = 5 per group). Red and green asterisks indicate statistically significant differences between 100 (green) or 300 (red) mg/kg/day NMN-administered and control mice by Wilcoxon matched-pairs singled-ranks test with Bonferroni adjusted p values (*p < 0.017, **p < 0.003).

(D and E) VO_2 (D) and EE (E) were compared between 6 and 12 months after NMN administration (6-month controls, black circles; 12-month controls, black triangles; 12-month 100 mg/kg/day NMN-administered mice, green triangles; 12-month 300 mg/kg/day NMN-administered mice, red triangles). Black, green, and red asterisks indicate statistically significant differences between controls at 6 and 12 months after NMN administration, between 100 mg/kg/day and control groups at 12 months, and between 300 mg/kg/day and control groups at 12 months of NMN treatment, respectively. Wilcoxon matched-pairs singled-ranks test with Bonferroni adjusted p values was used (*p < 0.01, **p < 0.002; n = 5 per group).

(F and G) Ambulations (F) and rearings (G) were measured for control (blue) and 100 (green) and 300 (red) mg/kg/day NMN-administered mice at 12–15 months of age. Hourly counts from 3 p.m. to 8 a.m. (left) and total counts during the dark time (6 p.m.–5 a.m., right) were presented. Red and green asterisks indicate statistically significant differences between 100 (green) or 300 (red) mg/kg/day NMN-administered and control mice by Wilcoxon matched-pairs singled-ranks test with Bonferroni adjusted p values (*p < 0.017, **p < 0.003; n = 9–10 per group). Black bars (A–E) and gray shaded areas (F and G) represent the dark period.

All values are presented as mean ± SEM.

observed even when all mice were included (Figure S4F). Consistent with this improved insulin sensitivity, intrahepatic triglyceride levels, a surrogate of insulin resistance, were lower in both NMN-administered groups at 6 months after and in the 300 mg/kg/day group at 12 months after NMN administration (Figure 4C). These results suggest that long-term NMN administration can ameliorate age-associated decline in insulin sensitivity, independent of its effect on body weight.

We also compared plasma concentrations of cholesterol, triglycerides, and free fatty acids (FFAs) among three groups. Plasma concentrations of cholesterol and triglycerides showed similar changes over time. For plasma FFA levels, the interaction between time and group was statistically significant (p = 0.007 from the two-way repeated-measures ANOVA), and the 300 mg/kg/day group did not show any statistically significant increases over time, whereas the control and the 100 mg/kg/day groups showed significant increases over time (p < 0.01 from tests of within-subjects effects in the one-way repeated-measures ANOVA). Indeed, plasma FFA levels tended to be lower in the 100 and 300 mg/kg groups compared to those in the control group at 9 and 12 months of NMN treatment, although the differences at each time point did not reach statistical significance (Figure 4D). This tendency appears to be consistent with lower respiratory quotient (Figure 3C), lower intrahepatic triglyceride levels (Figure 4C), and greater insulin sensitivity (Figure 4A) in NMN-administered mice, compared to the body-weight matched control mice.

Long-Term NMN Administration Reverses Age-Associated Gene Expression Changes in Peripheral Tissues and Enhances Mitochondrial Respiratory Capacity in Skeletal Muscle

Assessments of metabolic parameters in NMN-administered mice revealed significant effects of NMN to mitigate age-associated physiological decline. To further evaluate these anti-aging effects of NMN on molecular events, we conducted microarray analyses and compared global gene expression profiles in key metabolic organs including skeletal muscle, WAT, and the liver

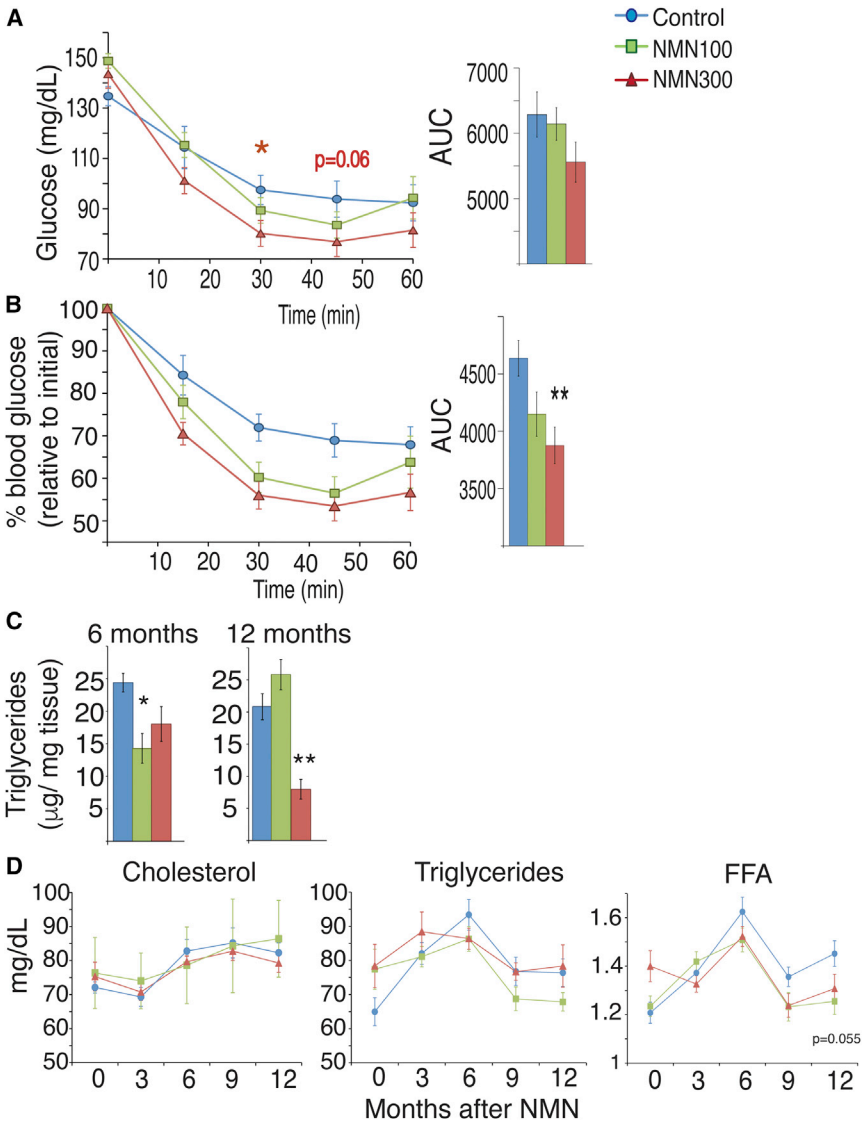

Figure 4. NMN-Administered Mice Show Improved Insulin Sensitivity and Lipid Profiles

Metabolic tests were performed after 12 months of their respective NMN doses. Results from control, 100, and 300 mg/kg/day NMN-administered mice are shown in blue, green, and red, respectively.

(A) Blood glucose levels were measured at the indicated times in insulin tolerance tests for body weight-matched mice after a 4 hr fast (n = 10–15 per group). Areas under the curves (AUCs) are also shown at right.

(B) Relative blood glucose levels were calculated for body weight-matched mice (n = 10–15 per group). Glucose levels at each time point are normalized to that at 0 min. AUCs are also shown at right.

(C) Intrahepatic triglyceride levels were measured after an overnight fast from animals in each group at 6 and 12 months after NMN administration (n = 4–5 per group).

(D) Plasma concentrations of cholesterol, triglycerides, and free fatty acids (FFA) were measured at 3, 6, 9, and 12 months of NMN treatment, after an overnight fast (n = 10–15 per group).

All values are presented as mean ± SEM. Asterisks indicate statistical significances compared to controls using one-way ANOVA (*$p < 0.05$; **$p < 0.01$).

between 6- and 12-month time points in each group of control and 300 mg/kg/day NMN-administered mice. Between 6 and 12 months of NMN treatment (11 and 17 months of age), 300, 360, and 513 genes were significantly changed in skeletal muscle, WAT, and the liver, respectively, in the control cohorts. Most of these genes were downregulated between these time points (Figure 5A). Remarkably, 76.3%, 73.1%, and 41.7% of the genes changed in skeletal muscle, WAT, and the liver of control mice, respectively, were not significantly altered in NMN-administered mice (Figure 5A), suggesting that NMN is able to prevent age-associated transcriptional changes in these three peripheral tissues. Nonetheless, among these three key metabolic tissues, no common genes were observed in top 20 genes based on the sum of the absolute values of *Z* ratios between two comparisons (*Z* difference) (Figure S5A), implying that the effect of NMN on transcription is tissue-specific. We also conducted parametric analysis of gene set enrichment (PAGE) and found that 55.5%, 54.4%, and 32.2% of biological pathways that show significant changes in skeletal muscle, WAT, and the liver of control mice, respectively, were not significantly altered in NMN-administered mice (Figure 5B). NMN affected diverse sets of biological pathways in these tissues, and no obvious common pathways were observed (Figure S4B). However, it should be noted that several WAT biological pathways related to immune function and inflammation were significantly upregulated in aged control mice, whereas these age-induced alterations were blunted in NMN-administered mice (e.g., CYTOKINE_ACTIVITY, LEUKOCYTE_ACTIVATION, IMMUNE_RESPONSE; Figure S5B), suggesting that NMN administration ameliorated age-associated increase in adipose tissue inflammation, a hallmark of obesity and insulin resistance (Berg and Scherer, 2005).

Next, we conducted principal component analysis (PCA) on the entire gene sets to further examine the global effects of NMN administration on age-associated transcriptional changes (Figure 5C). The first principal component (PC1) explained 20%–23% of the variance within the datasets and appeared to separate the expression profiles of young mice (blue and green) from those of old mice (red and orange) in skeletal muscle, WAT, and liver. Interestingly, compared to aged control mice (red), NMN-administered mice (orange) exhibited a shift toward young mice (blue and green) along the PC1 axis, particularly in skeletal muscle, supporting our notion that NMN administration prevents age-associated transcriptional changes.

Given that skeletal muscle exhibited the most profound preventive effects of NMN, we conducted high-resolution

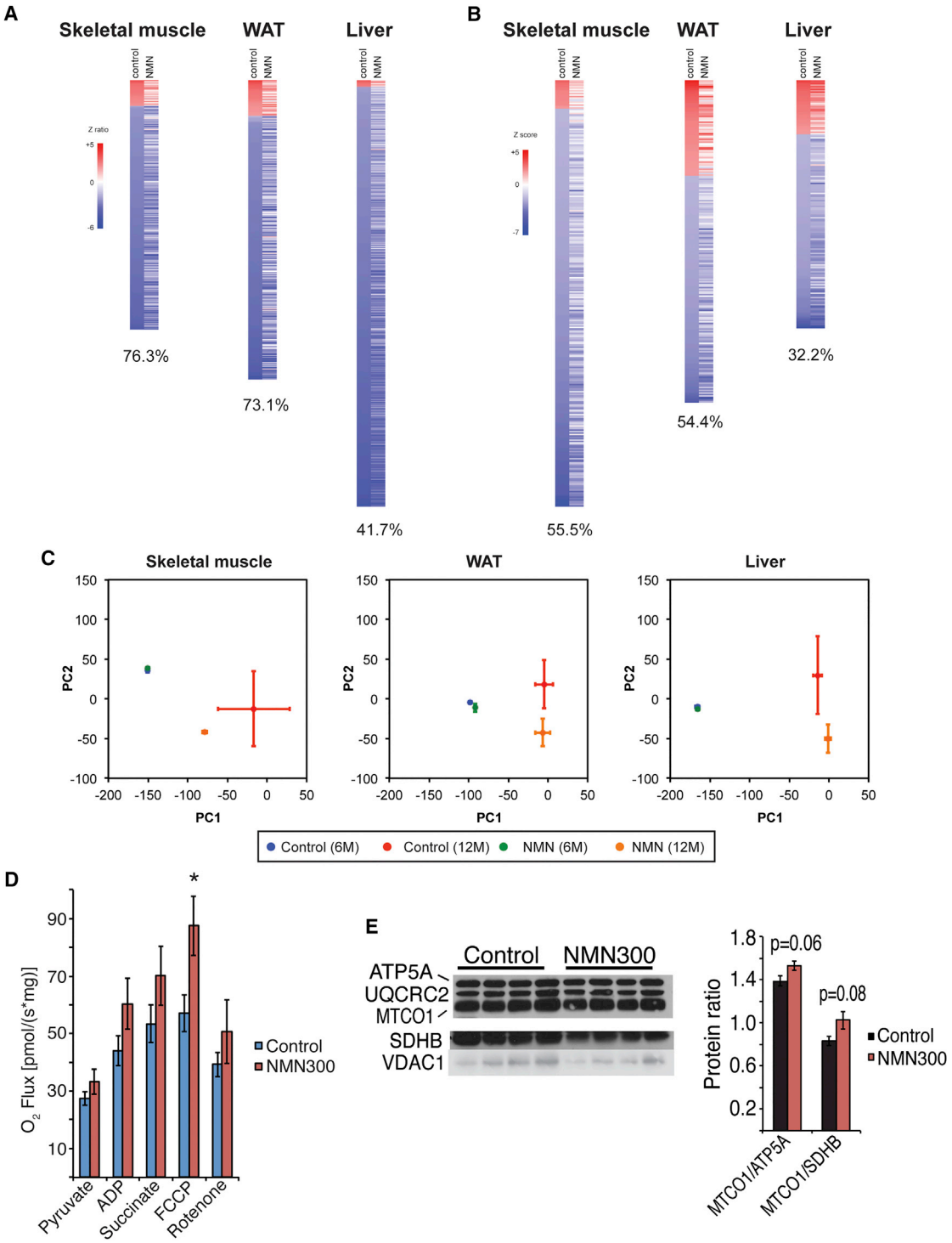

Figure 5. Long-Term NMN Administration Prevents Age-Associated Gene Expression Changes in Peripheral Tissues and Enhances Mitochondrial Respiratory Capacity in Skeletal Muscle

(A and B) Microarray analysis was conducted to compare gene expression profiles of skeletal muscle, white adipose tissue (WAT), and the liver in control and 300 mg/kg/day NMN-administered mice at 6 and 12 months after NMN administration. Throughout the figure, upregulated genes are shown in red and downregulated genes are shown in blue (n = 4 per group). Heatmaps in (A) reveal changes in individual gene expression. Genes that were significantly changed in control mice were selected by the rank product method (false discovery ratios [FDR] < 0.05) and ordered based on *Z* ratios of control mice. NMN administration inhibits age-induced changes in gene expression of skeletal muscle (76.3% of 300 genes), WAT (73.1% of 360 genes), and liver (41.7% of 513 genes). Heatmaps in (B) are shown from the parametric analysis of gene-set enrichment (PAGE). Biological pathways that were significantly changed in control mice were selected

(legend continued on next page)

respirometry on permeabilized skeletal muscles from control and 300 mg/kg/day NMN-treated mice. Skeletal muscle from NMN-treated mice showed significant enhancement of the maximum respiration rate induced by addition of a mitochondrial uncoupler FCCP and also a trend of increased mitochondrial oxidative metabolism stimulated by pyruvate, ADP, and succinate (Figure 5D), suggesting that NMN stimulates mitochondrial oxidative metabolism in skeletal muscle. Interestingly, NMN administration also increased the ratios of a mtDNA-encoded mitochondrial protein MTCO1 (cytochrome *c* oxidase subunit 1) and nuclear DNA-encoded mitochondrial proteins ATP5A (ATP synthase subunit 5α) or SDHB (succinate dehydrogenase complex subunit B) in mitochondrial extracts of skeletal muscle (Figure 5E), suggesting that NMN induces two critically correlated mitochondrial alterations, mitonuclear protein imbalance and mitochondrial oxidative metabolism, in skeletal muscle (Gomes et al., 2013; Houtkooper et al., 2013; Mouchiroud et al., 2013; van de Weijer et al., 2015). Taken together, these findings suggest that NMN mediates its anti-aging effect, at least in part, by preventing age-associated gene expression changes in a tissue-specific manner and also enhancing mitonuclear protein imbalance and mitochondrial oxidative metabolism in skeletal muscle.

Long-Term NMN Administration Significantly Improves Eye Function, Bone Density, and Myeloid-Lymphoid Composition in Aged Mice

In addition to metabolic functions, we assessed other pathophysiological changes in control and NMN-administered mice. The C57BL/6N mouse strain has been reported to carry the *rd8* mutation, a single nucleotide deletion in the *Crb1* gene (Mattapallil et al., 2012). This particular mutation causes the age-dependent accumulation of subretinal microglia and macrophages, which corresponds to the development of light-colored spots in the fundus of the eye (Aredo et al., 2015). Thus, we conducted fundus biomicroscopy for control and NMN-administered mice. Interestingly, whereas all five control C57BL/6N mice at 17 months of age showed many light-colored spots in their fundus, two and four out of five mice at 100 and 300 mg/kg/day doses, respectively, showed dramatic reduction in these spots, implicating that age-associated pathological changes caused by the *rd8* mutation may be suppressed by NMN in C57BL/6N mice (Figure 6A). In order to assess the effects of long-term NMN administration on retinal response, we conducted electroretinography (ERG). In the ERG analysis, there was a significant interaction between stimulus and group ($p = 0.009$ from the two-way repeated-measures ANOVA) for the scotopic a wave, and NMN-administered mice at both doses showed significantly higher amplitudes at 0 and 5 db ($p = 0.035$ and 0.022 for the 300 mg/kg group at 0 and 5 db, respectively; $p = 0.009$ for the 100 mg/kg group at 5 db from the Dunnett's T3 test in the one-way repeated-measures ANOVA within groups), suggesting that NMN is able to prevent the decline in rod cell function in aged C57BL/6N mice (Figure 6B). Furthermore, improvements for the scotopic b and phototic b waves, which represent Müller/bipolar cell function and cone cell function, respectively, were observed through entire ranges of stimulus in both 100 and 300 mg/kg/day groups (Figures 6C and 6D), although statistically significant interactions between stimulus and group were not achieved. Because the function of the lacrimal gland decreases with age in humans and rodents (Zoukhri, 2006), we also assessed tear production in control and NMN-administered mice with a modified Schirmer's test. Remarkably, NMN increased tear production in a dose-dependent manner at 12 months of NMN administration (Figure 6E). The tear production observed in the 300 mg/kg/day group was comparable to the maximal tear production throughout the mouse lifespan. In addition to these effects of NMN on eye function, we detected small but significant increases in bone density in NMN-administered mice in a dose-dependent manner (Figure 6F). NMN administration at both doses also significantly decreased the number of neutrophils, whereas it increases the number of lymphocytes at the dose of 300 mg/kg/day (Figures S2D–S2E). These additional findings provide support for our notion that NMN brings significant anti-aging effects on a variety of age-associated pathophysiological changes.

NMN Is Contained in Various Natural Foods

Finally, we found that NMN was indeed contained in some daily natural food sources (Table 1). For example, vegetables such as edamame (immature soybeans), broccoli, cucumber, and cabbage contained 0.25–1.88 mg of NMN per 100 g. Fruits such as avocado and tomato also contained 0.26–1.60 mg/100 g. Raw beef meat and shrimp contained relatively low levels of NMN (0.06–0.42 mg/100 g). Given that human red blood cells contain ~50 mg of NMN as a total (unpublished data), a physiologically relevant amount of NMN might be absorbed from various daily food sources to our body and help sustain NAD^+ biosynthesis and many physiological functions throughout the body.

DISCUSSION

In this study, we demonstrate that long-term administration of NMN is capable of mitigating age-associated physiological decline in regular chow-fed wild-type mice. We found that a 12-month-long NMN administration (1) is well-tolerated without

by PAGE ($p < 0.05$) and ordered based on *Z* scores of control mice. NMN administration inhibits these age-induced changes in pathways of skeletal muscle (55.5% of 299 pathways), WAT (54.4% of 226 pathways), and liver (32.2% of 174 pathways).

(C) Principal component analysis (PCA) was performed on the entire gene sets. The x and y axes indicate the first and the second principal components (PC1 and PC2), respectively. All values are presented as mean ± SEM (n = 4).

(D) High-resolution respirometry was performed for permeabilized skeletal muscles from control (n = 7) and 300 mg/kg/day NMN-treated (NMN300; n = 9) mice at 6 months. Mitochondrial oxidative respiration was measured by addition of pyruvate, ADP, succinate, a mitochondrial uncoupler FCCP, and a complex I inhibitor rotenone.

(E) Protein levels of nuclear DNA-encoded and mtDNA-encoded mitochondrial proteins (ATP5A, UQCRC2, SDHB, and VDAC1 versus MTCO1, respectively) were measured in mitochondrial extracts from control and 300 mg/kg/day NMN-treated skeletal muscles at 6 months (left panel; n = 4). The protein ratios of MTCO1 to ATP5A or SDHB were calculated by quantitating signal intensities of each band (right panel). All values are presented as mean ± SEM.

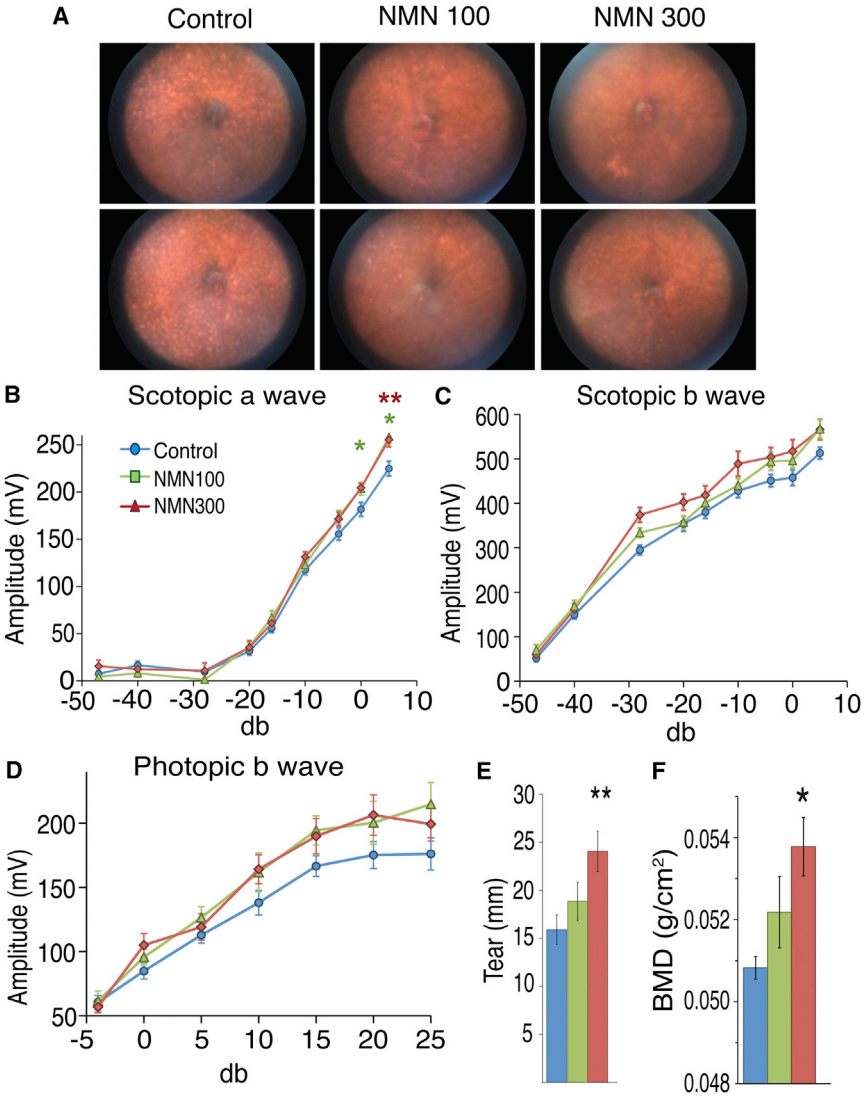

Figure 6. Long-Term NMN Administration Significantly Improves Eye Function, Tear Production, and Bone Mineral Density in Aged C57BL/6N Mice

Eye function and bone density were analyzed after 12 months of NMN administration (at 17 months of age). Results from control and 100 and 300 mg/kg/day NMN-administered mice are shown in blue, green, and red, respectively.

(A) Representative fundus biomicroscopy photos from control, 100, and 300 mg/kg/day NMN-administered mice (n = 5 per group). Light-colored spots due to the *rd8* mutation carried by C57BL/6N mice were seen in all five control mice. Two and four out of five mice at 100 and 300 mg/kg/day, respectively, showed dramatic reductions in these spots.

(B–D) Scotopic a (B), scotopic b (C), and photopic b (D) waves were measured by electroretinography (ERG) and analyzed using two-way RANOVA with Dunnett's T3 post hoc test (n = 10–24 per group).

(E) Tear production was assessed using a modified Schirmer's test and analyzed by one-way ANOVA (n = 20 per group).

(F) Bone mineral density (BMD) was evaluated by dual-energy X-ray absorptiometry (DEXA) and analyzed by one-way ANOVA (n = 4–5 per group).

All values are presented as mean ± SEM. Asterisks indicate statistical significances compared to controls (*$p < 0.05$; **$p < 0.01$).

any obvious deleterious effects, (2) suppresses age-associated body weight gain, (3) enhances food intake, oxygen consumption, energy expenditure, and physical activity, (4) improves insulin sensitivity and plasma lipid profile, independent of its effect on body weight, and (5) improves eye function, bone density, and myeloid-lymphoid composition. NMN administration was also able to prevent age-associated gene expression changes in a tissue-dependent manner and enhance mitochondrial respiratory capability in skeletal muscle. In addition to the already reported effects of short-term NMN administration on various pathological conditions (Caton et al., 2011; Gomes et al., 2013; Long et al., 2015; Stein and Imai, 2014; Yamamoto et al., 2014; Yoshino et al., 2011), this pleiotropic effect of long-term NMN administration opens a new avenue to develop effective anti-aging interventions using key NAD^+ intermediates such as NMN.

A number of studies have reported that NAD^+ availability decreases throughout the body in mice and humans over age (Gomes et al., 2013; Massudi et al., 2012; Mouchiroud et al., 2013; Stein and Imai, 2014; Yoshino et al., 2011; Zhu et al., 2015). Given that key NAD^+-consuming enzymes, such as sirtuins, poly-ADP-ribose polymerases (PARPs), and CD38/157 ectoenzymes, play critical roles in many biological processes including metabolism, inflammation, and stress and damage response (Cantó et al., 2015; Imai and Guarente, 2014), such global decreases in NAD^+ availability could result in serious physiological decline over age. Thus, enhancing NAD^+ biosynthesis by using NAD^+ intermediates, such as NMN and NR, is expected to be able to ameliorate such age-associated physiological decline effectively. Indeed, the beneficial anti-aging effect of NMN has been predicted in the concept of the "NAD World," a hypothetical systemic regulatory network for the control of aging and longevity in mammals (Imai, 2009, 2011). Our new findings from this long-term NMN administration study clearly provide strong support to this prediction by the NAD World concept and put a significant emphasis on the importance of NAD^+ decrease as a common trigger of age-associated physiological decline.

It should be noted that NMN administration did not generate any obvious toxicity, serious side effects, or increased mortality rate throughout the 12-month-long intervention period, suggesting the long-term safety of NMN. Nonetheless, an optimal dose of NMN to maximize its efficacy appears to differ depending on physiological functions. For example, whereas the effects of NMN on body weight gain, insulin sensitivity, tear production, and bone mineral density were dose-dependent, 100 mg/kg/day of NMN improved oxygen consumption, energy expenditure, and physical activity better than 300 mg/kg/day. For rod

Table 1. NMN Is Present in Various Types of Natural Food

Food Type	Name	mg/100 g-Food
Vegetable	edamame	0.47–1.88
Vegetable	broccoli	0.25–1.12
Vegetable	cucumber seed	0.56
	cucumber peel	0.65
Vegetable	cabbage	0.0–0.90
Fruit	avocado	0.36–1.60
Fruit	tomato	0.26–0.30
Other	mushroom	0.0–1.01
Meat	beef (raw)	0.06–0.42
Seafood	shrimp	0.22

NMN was extracted from each food and measured by HPLC. Several different sources were examined for some foods, showing ranges of values.

and cone photoreceptor function, both doses had similar effects. Indeed, we found that expression of *Ox2r* and *Prdm13*, two downstream genes in the SIRT1-mediated signaling pathway in the hypothalamus, exhibited significant decreases in the hypothalami of 300 mg/kg/day NMN-treated mice (our preliminary finding), which could partly explain some of the observed differences in the effects of NMN, particularly those on physical activity, between two tested doses. Additionally, the extent of age-dependent NAD^+ decline or NMN uptake in each tissue or organ might determine an optimal dose of NMN to restore each physiological function. Given that 100 mg/kg/day of NMN was able to mitigate most age-associated physiological declines in mice, an equivalent surface area dose for humans would be ~8 mg/kg/day (Freireich et al., 1966), providing hope to translate our findings to humans.

Detailed molecular mechanisms responsible for the pleiotropic effects of NMN need to be investigated further. Nonetheless, our analyses of global gene expression profiles in skeletal muscle, WAT, and the liver revealed that NMN administration was able to prevent age-associated transcriptional changes in a tissue-specific manner. In particular, skeletal muscle exhibited the most profound preventive effects of NMN on age-associated transcriptional changes. Consistent with this finding, mitochondrial oxidative metabolism was significantly enhanced in NMN-treated skeletal muscle. Additionally, NMN-treated skeletal muscle showed enhanced mitonuclear protein imbalance (Houtkooper et al., 2013; Mouchiroud et al., 2013), which has recently been reported to correlate to enhanced NAD^+ biosynthesis and mitochondrial oxidative metabolism in human skeletal muscle (van de Weijer et al., 2015). Thus, it is likely that skeletal muscle is one of the most sensitive target tissues for the anti-aging effects of NMN. One would also suspect that some of the anti-aging effects of NMN administration might be modified by the function of SIRT1 in the brain, particularly in the hypothalamus (Satoh et al., 2013; Yoon et al., 2015). Other nuclear and mitochondrial sirtuins, such as SIRT6 and SIRT3-5, might mediate these pleiotropic effects of NMN in a tissue-dependent manner. It is also possible that target organs and mediators causing the effects of long-term NMN administration might not be the same as those causing the effects of acute NMN administration (Gomes et al., 2013; Yoshino et al., 2011). Therefore, further careful investigation will be necessary to identify major target organs and effector molecules for each effect of NMN administration at different time points.

Our present study clearly shows that NMN is quickly absorbed from the gut into blood circulation within 2–3 min and also cleared from blood circulation into tissues within 15 min. The isotopic tracing experiment with C13-D-NMN also confirmed this fast absorption of NMN and its immediate conversion to NAD^+ in tissues. These in vivo pharmacokinetic data imply that there may be an effective transporter that directly uptakes NMN into cells and tissues. Similarly, it has been suggested that NR is directly transported into cells through nucleoside transporters (Nikiforov et al., 2011). Taken together, studying in vivo pharmacokinetics and identifying precise mechanisms responsible of NMN and NR uptake will provide critical insight into understanding tissue preferences of these two distinct NAD^+ precursors and thereby developing effective interventions for age-associated physiological decline by using NMN, NR, or their combination.

In conclusion, our long-term NMN administration study provides compelling support to an effective anti-aging intervention using NMN, a key NAD^+ intermediate. Given that NMN is contained in a variety of food sources such as vegetables, fruits, and meat, it will be of great interest to translate our study from mice to humans and examine whether this endogenous compound, NMN, is also an effective intervention that prevents age-associated physiological decline in humans.

EXPERIMENTAL PROCEDURES

Animal Experimentation

C57BL/6N male mice (Taconic, NY) were group-housed in a barrier facility with 12-hr light/12-hr dark cycles. All mice received a regular chow diet ad libitum (PicoLab 5053 Rodent Diet 20; Lab Diets). Body weights were measured weekly at the same time each week. Food and water intake were measured once every month for 3–7 consecutive days at the same time each month. Fed and fasted blood samples were collected monthly at the same time each month as described previously (Revollo et al., 2007) and used for glucose, insulin, blood cell counts, and lipid analysis (Yoshino et al., 2011). IPGTTs and ITTs were conducted throughout morning and early afternoon after fasting for 16–18 hr and 4 hr, respectively, once before NMN administration began and every 3 months thereafter, as described previously (Yoshino et al., 2011). Metabolic parameters were measured after 6 and 12 months of NMN administration using an Oxymax indirect calorimetry system (Columbus Instruments). Rectal body temperature was measured monthly, as described previously (Satoh et al., 2010). Urine, whole blood samples, histopathology, and bone mineral density were analyzed after 12 months of NMN treatment. Tissue samples were collected every 3 months from mice not subjected to invasive tests and used for NAD^+ measurement, microarray, and other analyses. All animal studies were approved by the Washington University Animal Studies Committee and were in accordance with NIH guidelines. Details are available in the Supplemental Experimental Procedures.

Long-Term NMN Administration

Water consumption was measured for 2 weeks prior to the start of NMN administration. NMN was generated and obtained from the Oriental Yeast Co. Purity of NMN, evaluated by HPLC, was 96%–97%, and the endotoxin level was 0.1–0.2 EU/mg. NMN was then administered in drinking water ad libitum at either 100 or 300 mg/kg/day, based on the previously measured water consumption. The administration began at 5 months of age and continued for 12 months, until they became 17 months old. The NMN solution was prepared weekly in small batches by dissolving NMN into autoclaved water at the respective doses and filtering sterilely. Aliquots were collected from each

batch and measured by HPLC to confirm stability of the compound. Water bottles and cages were changed twice weekly.

Oral Gavage and Measurements of NMN and NAD+

Three-month-old C57BL/6N male mice (Taconic) received NMN (300 mg/kg) or PBS orally after an overnight fast. Blood was collected from the tail vein after 0, 2, 5, 10, 15, and 30 min, and plasma was separated by centrifugation. Tissue samples were collected at 0, 5, 15, 30, and 60 min time points after gavage of NMN (300 mg/kg) or PBS. Plasma NMN and tissue NAD^+ levels were determined using a HPLC system (Shimadzu) with a Hypercarb column (15 cm × 4.6 cm; Thermo Scientific) and a Supelco LC-18-T column (15 cm × 4.6 cm; Sigma), respectively, as described previously (Yoshino et al., 2011).

Microarrays

Total RNA was isolated from frozen skeletal muscle, white adipose tissue (WAT), and liver samples of control and NMN-treated mice at the age of 11 and 17 months (6 and 12 months intervention period, respectively) using the PureLink RNA Mini Kit (Invitrogen). To determine global transcriptional changes induced by aging in control and NMN-treated mice, we conducted microarray study using the Illumina Mouse Ref 8 whole genome microarrays (version 2). All microarray data have been deposited to the GEO database (GEO: GSE85718; https://www.ncbi.nlm.nih.gov/geo/). Details are available in the Supplemental Experimental Procedures.

High-Resolution Respirometry

Oxygen consumption was measured using the Oroboros High-Resolution Respirometry System in the Adipocyte Biology and Molecular Nutrition Core at Washington University. The soleus muscle (~25 mg) was immediately removed from mice with minimal separation of the fibers and used for the assay. Details are available in the Supplemental Experimental Procedures.

Western Blotting of Mitochondrial Extracts

Skeletal muscles were dissected between 9 and 11 p.m., and mitochondrial extracts were prepared from soleus muscle. Details are available in the Supplemental Experimental Procedures.

Statistical Analyses

Differences between two groups were assessed using the Student's t test. Comparisons among several groups were performed using repeated-measures ANOVA or one-way ANOVA with various post hoc tests indicated in the text or figure legends. Dose dependency was determined with one-way ANOVA with the unweighted linear term. Wilcoxon matched-pairs singled-ranks test was used to compare differences in oxygen consumption, energy expenditure, respiratory quotient, and physical activity, and the Bonferroni correction was applied to calculate adjusted p values. For other comparisons, p values ≤ 0.05 were considered statistically significant. We used Microsoft Excel 2008 and SPSS (Version 22 and 23) to conduct statistical analyses.

ACCESSION NUMBERS

The accession number for the microarray data reported in this paper is GEO: GSE85718.

SUPPLEMENTAL INFORMATION

Supplemental Information includes Supplemental Experimental Procedures and five figures and can be found with this article online at http://dx.doi.org/10.1016/j.cmet.2016.09.013.

AUTHOR CONTRIBUTIONS

S.I. and J.Y. conceived and supervised the entire study. K.F.M., L.R.S., J.Y., and S.I. designed the experiments. K.F.M. performed most of the experiments. J.Y. and L.R.S. conducted microarray analyses and physical activity measurements, respectively. S.K. and R.S.A. conducted and analyzed eye function and tear production. P.R. and M.M. provided isotopic NMN. A.G. and Y.S. conducted isotopic tracing experiments. S.Y. and K.U. produced NMN for this entire study. K.F.M., L.R.S., A.G., J.Y., and S.I. analyzed the data and wrote the manuscript.

ACKNOWLEDGMENTS

We thank Sunnie Hsiung, Megan Hurt-Arb, and Terri Pietka for their technical assistance. We also thank late Toshikuni Naito, Ryuji Nakamura, Masashi Nakagawa, Hideo Arai, Ken Kanzaki, Hisataka Yasuda, and Yoshifumi Masuda in Oriental Yeast Co. for their support to this sponsored research project, Kazuo Tsubota and Takaaki Inaba at Keio University School of Medicine for their technical support for tear production measurement, Mr. Tsunemaru Tanaka and Ms. Megumi Tanaka for their generous gift of NMN, members of the S.I. lab for critical comments and suggestions on this study, and staff members in the core facilities provided by the Diabetes Research Center (P30 DK020579), Nutrition Obesity Research Center (P30 DK56341), a Research to Prevent Blindness Physician Scientist Award (R.S.A.) and a Research to Prevent Blindness Unrestricted Grant to Department of Ophthalmology, and the Hope Center for Neurological Disorders at Washington University. M.E.M. is supported by the Biotechnology and Biological Science Research Council (BBSRC; BB/N001842/1). This work was conducted thoroughly under a sponsored research agreement between Washington University and Oriental Yeast Co. R.S.A. is a co-founder of Metro Midwest Biotech, and M.E.M. serves as a consultant for ChromaDex.

Received: December 4, 2015
Revised: July 5, 2016
Accepted: September 24, 2016
Published: October 27, 2016

REFERENCES

Anderson, R.M., Bitterman, K.J., Wood, J.G., Medvedik, O., Cohen, H., Lin, S.S., Manchester, J.K., Gordon, J.I., and Sinclair, D.A. (2002). Manipulation of a nuclear NAD+ salvage pathway delays aging without altering steady-state NAD+ levels. J. Biol. Chem. *277*, 18881–18890.

Aredo, B., Zhang, K., Chen, X., Wang, C.X., Li, T., and Ufret-Vincenty, R.L. (2015). Differences in the distribution, phenotype and gene expression of subretinal microglia/macrophages in C57BL/6N (Crb1 rd8/rd8) versus C57BL6/J (Crb1 wt/wt) mice. J. Neuroinflammation *12*, 6.

Balan, V., Miller, G.S., Kaplun, L., Balan, K., Chong, Z.Z., Li, F., Kaplun, A., VanBerkum, M.F., Arking, R., Freeman, D.C., et al. (2008). Life span extension and neuronal cell protection by Drosophila nicotinamidase. J. Biol. Chem. *283*, 27810–27819.

Barzilai, N., Crandall, J.P., Kritchevsky, S.B., and Espeland, M.A. (2016). Metformin as a Tool to Target Aging. Cell Metab. *23*, 1060–1065.

Belenky, P., Racette, F.G., Bogan, K.L., McClure, J.M., Smith, J.S., and Brenner, C. (2007). Nicotinamide riboside promotes Sir2 silencing and extends lifespan via Nrk and Urh1/Pnp1/Meu1 pathways to NAD^+. Cell *129*, 473–484.

Berg, A.H., and Scherer, P.E. (2005). Adipose tissue, inflammation, and cardiovascular disease. Circ. Res. *96*, 939–949.

Brown, K.D., Maqsood, S., Huang, J.Y., Pan, Y., Harkcom, W., Li, W., Sauve, A., Verdin, E., and Jaffrey, S.R. (2014). Activation of SIRT3 by the NAD^+ precursor nicotinamide riboside protects from noise-induced hearing loss. Cell Metab. *20*, 1059–1068.

Cantó, C., Houtkooper, R.H., Pirinen, E., Youn, D.Y., Oosterveer, M.H., Cen, Y., Fernandez-Marcos, P.J., Yamamoto, H., Andreux, P.A., Cettour-Rose, P., et al. (2012). The NAD(+) precursor nicotinamide riboside enhances oxidative metabolism and protects against high-fat diet-induced obesity. Cell Metab. *15*, 838–847.

Cantó, C., Menzies, K.J., and Auwerx, J. (2015). NAD(+) metabolism and the control of energy homeostasis: a balancing act between mitochondria and the nucleus. Cell Metab. *22*, 31–53.

Caton, P.W., Kieswich, J., Yaqoob, M.M., Holness, M.J., and Sugden, M.C. (2011). Nicotinamide mononucleotide protects against pro-inflammatory cytokine-mediated impairment of mouse islet function. Diabetologia *54*, 3083–3092.

Cerutti, R., Pirinen, E., Lamperti, C., Marchet, S., Sauve, A.A., Li, W., Leoni, V., Schon, E.A., Dantzer, F., Auwerx, J., et al. (2014). NAD(+)-dependent activation of Sirt1 corrects the phenotype in a mouse model of mitochondrial disease. Cell Metab. *19*, 1042–1049.

de Picciotto, N.E., Gano, L.B., Johnson, L.C., Martens, C.R., Sindler, A.L., Mills, K.F., Imai, S., and Seals, D.R. (2016). Nicotinamide mononucleotide supplementation reverses vascular dysfunction and oxidative stress with aging in mice. Aging Cell *15*, 522–530.

Freireich, E.J., Gehan, E.A., Rall, D.P., Schmidt, L.H., and Skipper, H.E. (1966). Quantitative comparison of toxicity of anticancer agents in mouse, rat, hamster, dog, monkey, and man. Cancer Chemother. Rep. *50*, 219–244.

Gariani, K., Menzies, K.J., Ryu, D., Wegner, C.J., Wang, X., Ropelle, E.R., Moullan, N., Zhang, H., Perino, A., Lemos, V., et al. (2015). Eliciting the mitochondrial unfolded protein response via NAD repletion reverses fatty liver disease. Hepatology *63*, 1190–1204.

Gomes, A.P., Price, N.L., Ling, A.J., Moslehi, J.J., Montgomery, M.K., Rajman, L., White, J.P., Teodoro, J.S., Wrann, C.D., Hubbard, B.P., et al. (2013). Declining NAD(+) induces a pseudohypoxic state disrupting nuclear-mitochondrial communication during aging. Cell *155*, 1624–1638.

Gong, B., Pan, Y., Vempati, P., Zhao, W., Knable, L., Ho, L., Wang, J., Sastre, M., Ono, K., Sauve, A.A., and Pasinetti, G.M. (2013). Nicotinamide riboside restores cognition through an upregulation of proliferator-activated receptor-γ coactivator 1α regulated β-secretase 1 degradation and mitochondrial gene expression in Alzheimer's mouse models. Neurobiol. Aging *34*, 1581–1588.

Houtkooper, R.H., Mouchiroud, L., Ryu, D., Moullan, N., Katsyuba, E., Knott, G., Williams, R.W., and Auwerx, J. (2013). Mitonuclear protein imbalance as a conserved longevity mechanism. Nature *497*, 451–457.

Hubbard, B.P., and Sinclair, D.A. (2014). Small molecule SIRT1 activators for the treatment of aging and age-related diseases. Trends Pharmacol. Sci. *35*, 146–154.

Imai, S. (2009). The NAD World: a new systemic regulatory network for metabolism and aging–Sirt1, systemic NAD biosynthesis, and their importance. Cell Biochem. Biophys. *53*, 65–74.

Imai, S. (2010). A possibility of nutriceuticals as an anti-aging intervention: activation of sirtuins by promoting mammalian NAD biosynthesis. Pharmacol. Res. *62*, 42–47.

Imai, S. (2011). Dissecting systemic control of metabolism and aging in the NAD World: the importance of SIRT1 and NAMPT-mediated NAD biosynthesis. FEBS Lett. *585*, 1657–1662.

Imai, S., and Guarente, L. (2014). NAD+ and sirtuins in aging and disease. Trends Cell Biol. *24*, 464–471.

Khan, N.A., Auranen, M., Paetau, I., Pirinen, E., Euro, L., Forsström, S., Pasila, L., Velagapudi, V., Carroll, C.J., Auwerx, J., and Suomalainen, A. (2014). Effective treatment of mitochondrial myopathy by nicotinamide riboside, a vitamin B3. EMBO Mol. Med. *6*, 721–731.

Lamming, D.W., Ye, L., Sabatini, D.M., and Baur, J.A. (2013). Rapalogs and mTOR inhibitors as anti-aging therapeutics. J. Clin. Invest. *123*, 980–989.

Lee, H.J., Hong, Y.S., Jun, W., and Yang, S.J. (2015). Nicotinamide riboside ameliorates hepatic metaflammation by modulating NLRP3 inflammasome in a rodent model of type 2 diabetes. J. Med. Food *18*, 1207–1213.

Long, A.N., Owens, K., Schlappal, A.E., Kristian, T., Fishman, P.S., and Schuh, R.A. (2015). Effect of nicotinamide mononucleotide on brain mitochondrial respiratory deficits in an Alzheimer's disease-relevant murine model. BMC Neurol. *15*, 19.

Massudi, H., Grant, R., Braidy, N., Guest, J., Farnsworth, B., and Guillemin, G.J. (2012). Age-associated changes in oxidative stress and NAD+ metabolism in human tissue. PLoS ONE *7*, e42357.

Mattapallil, M.J., Wawrousek, E.F., Chan, C.C., Zhao, H., Roychoudhury, J., Ferguson, T.A., and Caspi, R.R. (2012). The Rd8 mutation of the Crb1 gene is present in vendor lines of C57BL/6N mice and embryonic stem cells, and confounds ocular induced mutant phenotypes. Invest. Ophthalmol. Vis. Sci. *53*, 2921–2927.

Mouchiroud, L., Houtkooper, R.H., Moullan, N., Katsyuba, E., Ryu, D., Cantó, C., Mottis, A., Jo, Y.S., Viswanathan, M., Schoonjans, K., et al. (2013). The NAD(+)/sirtuin pathway modulates longevity through activation of mitochondrial UPR and FOXO signaling. Cell *154*, 430–441.

Nikiforov, A., Doelle, C., Niere, M., and Ziegler, M. (2011). Pathways and subcellular compartmentation of NAD biosynthesis in human cells: from entry of extracellular precursors to mitochondrial NAD generation. J. Biol. Chem. *286*, 21767–21778.

OECD (2013). In What Future for Health Spending?, O.E. Department, ed. (Paris, France: Organisation for Economic Co-operation and Development).

Ramsey, K.M., Mills, K.F., Satoh, A., and Imai, S. (2008). Age-associated loss of Sirt1-mediated enhancement of glucose-stimulated insulin secretion in β cell-specific Sirt1-overexpressing (BESTO) mice. Aging Cell *7*, 78–88.

Revollo, J.R., Körner, A., Mills, K.F., Satoh, A., Wang, T., Garten, A., Dasgupta, B., Sasaki, Y., Wolberger, C., Townsend, R.R., et al. (2007). Nampt/PBEF/Visfatin regulates insulin secretion in β cells as a systemic NAD biosynthetic enzyme. Cell Metab. *6*, 363–375.

Satoh, A., Brace, C.S., Ben-Josef, G., West, T., Wozniak, D.F., Holtzman, D.M., Herzog, E.D., and Imai, S. (2010). SIRT1 promotes the central adaptive response to diet restriction through activation of the dorsomedial and lateral nuclei of the hypothalamus. J. Neurosci. *30*, 10220–10232.

Satoh, A., Brace, C.S., Rensing, N., Cliften, P., Wozniak, D.F., Herzog, E.D., Yamada, K.A., and Imai, S. (2013). Sirt1 extends life span and delays aging in mice through the regulation of Nk2 homeobox 1 in the DMH and LH. Cell Metab. *18*, 416–430.

Stein, L.R., and Imai, S. (2014). Specific ablation of Nampt in adult neural stem cells recapitulates their functional defects during aging. EMBO J. *33*, 1321–1340.

Tummala, K.S., Gomes, A.L., Yilmaz, M., Graña, O., Bakiri, L., Ruppen, I., Ximénez-Embún, P., Sheshappanavar, V., Rodriguez-Justo, M., Pisano, D.G., et al. (2014). Inhibition of de novo NAD(+) synthesis by oncogenic URI causes liver tumorigenesis through DNA damage. Cancer Cell *26*, 826–839.

van de Weijer, T., Phielix, E., Bilet, L., Williams, E.G., Ropelle, E.R., Bierwagen, A., Livingstone, R., Nowotny, P., Sparks, L.M., Paglialunga, S., et al. (2015). Evidence for a direct effect of the NAD+ precursor acipimox on muscle mitochondrial function in humans. Diabetes *64*, 1193–1201.

Wang, X., Hu, X., Yang, Y., Takata, T., and Sakurai, T. (2016). Nicotinamide mononucleotide protects against β-amyloid oligomer-induced cognitive impairment and neuronal death. Brain Res. *1643*, 1–9.

Yamamoto, T., Byun, J., Zhai, P., Ikeda, Y., Oka, S., and Sadoshima, J. (2014). Nicotinamide mononucleotide, an intermediate of NAD+ synthesis, protects the heart from ischemia and reperfusion. PLoS ONE *9*, e98972.

Yoon, M.J., Yoshida, M., Johnson, S., Takikawa, A., Usui, I., Tobe, K., Nakagawa, T., Yoshino, J., and Imai, S. (2015). SIRT1-mediated eNAMPT secretion from adipose tissue regulates hypothalamic NAD+ and function in mice. Cell Metab. *21*, 706–717.

Yoshino, J., Mills, K.F., Yoon, M.J., and Imai, S. (2011). Nicotinamide mononucleotide, a key NAD(+) intermediate, treats the pathophysiology of diet- and age-induced diabetes in mice. Cell Metab. *14*, 528–536.

Zhang, H., Ryu, D., Wu, Y., Gariani, K., Wang, X., Luan, P., D'Amico, D., Ropelle, E.R., Lutolf, M.P., Aebersold, R., et al. (2016). NAD^+ repletion improves mitochondrial and stem cell function and enhances life span in mice. Science *352*, 1436–1443.

Zhu, X.H., Lu, M., Lee, B.Y., Ugurbil, K., and Chen, W. (2015). In vivo NAD assay reveals the intracellular NAD contents and redox state in healthy human brain and their age dependences. Proc. Natl. Acad. Sci. USA *112*, 2876–2881.

Zoukhri, D. (2006). Effect of inflammation on lacrimal gland function. Exp. Eye Res. *82*, 885–898.